Γ-X mixing effect in GaAs/AlAs superlattices and heterojunctions

Jian-Bai Xia
China Center of Advanced Science and Technology (World Laboratory), P.O. Box 8730, Beijing 100080, China
and Institute of Semiconductors, Chinese Academy of Sciences, P.O. Box 912, Beijing 100083, China
(Received 20 July 1989)

The Γ-X mixing effect on the subband structure of superlattice $(GaAs)_{12}/(AlAs)_{12}$ is investigated with both the pseudopotential method and the effective-mass method. The results derived from the two methods show reasonable agreement, and the best-fitting Γ-X scattering parameter t is determined to be 0.5. The transmission probabilities of the Γ-point electron through the bound X-point states in the AlAs layer are calculated quantitatively. It is found that the resonant peaks correspond completely to the eigenstates of the corresponding superlattice, and the Γ-resonant peak is relatively smaller than the X-resonant peaks. Under the applied electric field, the resonant peaks originating from two barriers separate, resulting in a reduction of the peak-to-valley ratio.

I. INTRODUCTION

The Γ-X mixing effect in $GaAs/Al_xGa_{1-x}As$ quantum wells has been verified experimentally for the first time in resonant tunneling of high-energy states by Mendez *et al.*[1] Experiments showed well-defined features in the current-voltage characteristics, corresponding to energies above the well barrier, which are interpreted as resulting from resonant tunneling through confined states in $Al_xGa_{1-x}As$ at the high-symmetry X point of the Brillouin zone.

Before the experiment of Mendez *et al.*,[1] Osbourn[2] and Maihiot *et al.*[3] had theoretically predicted this phenomenon in GaAs/strained-$Ga_{1-x}As_xP$/GaAs and $GaAs/Al_xGa_{1-x}As$/GaAs (100) double heterojunctions. In these two cases the materials of potential barrier are all of indirect energy gap. They found that under energetically favorable conditions, the transport behavior exhibits very sharp resonance scattering through available propagating X-point states, and has large transmission probabilities. This phononless intervalley scattering at the interface, so called by Osbourn,[2] has very small probability except for the resonant condition.

This kind of scattering cannot be taken into account by the usual effective-mass theory; however, Ando and Akera[4] presented a formulation in which Γ-X mixings at interfaces can be treated within the framework of the effective-mass approximation. They introduced an interface matrix describing boundary conditions for the Γ valley and the X valley, and determined the interface matrix by calculating nearest-neighbor transfer integrals[5] with an empirical tight-binding model.

The Γ-X mixing effect exists not only in the resonant-tunneling process, but also in the electronic subband structure of the short-period superlattice GaAs/AlAs. Pseudopotential calculations[6,7] showed that for the layer number n smaller than a certain value (for example, 8 or 10), the superlattice $(GaAs)_n/(AlAs)_n$ has an indirect energy gap with a lowest electronic energy level of X character. The photoluminescence measurements of short-period superlattices $(GaAs)_n/(AlAs)_n$ under hydrostatic pressure[8] indicated that at room temperature the Γ- and X-point energy levels cross for $n=11$. It is obvious that at the crossing the Γ- and X-point energy levels will interact with each other, resulting in the hybridization of states. Lu and Sham[9] studied the valley-mixing effects in short-period superlattices with use of a second-neighbor tight-binding method.

Besides the above works, there were also works on resonant tunneling through GaAs quantum-well energy levels confined by $Al_xGa_{1-x}As$ Γ- and X-point barriers,[10] and the experimental[11] and theoretical[12] investigations of the Fowler-Nordheim tunneling process in which electrons are scattered between the Γ minimum and the four lateral X minima by the alloy disorder.

In this paper we study the Γ-X mixing effect on both subband structures of short-period superlattices and the resonant tunneling of heterojunctions. First, we use the pseudopotential method[7,13] and Ando's effective-mass model to calculate the interaction and hybridization of Γ- and X-point energy levels in the superlattice $(GaAs)_{12}/(AlAs)_{12}$, in which they are assumed to cross. By comparing the results derived from the two models, the best-fitting parameter in the interface matrix is determined. Then we apply the effective-mass model with the interface matrix to calculate the tunneling transmission probabilities for various cases. Sections II and III are the Γ-X mixing effect on the subband structure of superlattices studied by the pseudopotential method and effective-mass method, respectively. Section IV is the Γ-X mixing effect on resonant tunneling of heterojunctions.

II. Γ-X MIXING EFFECT ON SUBBAND STRUCTURE STUDIED WITH THE PSEUDOPOTENTIAL METHOD

The pseudopotential method used to calculate the subband structure of superlattices has been described elsewhere.[7,13] Here we outline the main points as follows. Pseudopotential calculations are carried out by a two-step procedure. In the first step, a usual pseudopotential calculation is made for an average lattice, with pseudopo-

tentials which are weighted averages of the pseudopotentials of the component materials. In the second step, the Bloch solutions obtained in the first step are used as a new basis in the calculation for the superlattice,

$$\psi(\mathbf{r})=\sum_{l,\mathbf{k}_i} c_{li}\psi_{l\mathbf{k}_i}(\mathbf{r}) , \tag{1}$$

where $\psi_{l\mathbf{k}_i}(\mathbf{r})$ are the Bloch solutions with wave vectors,

$$\mathbf{k}_i=(\mathbf{k}_{\parallel},2\pi i/L) ,$$
$$i=-N+1,-N+2,\ldots,0,\ldots,N-1,N . \tag{2}$$

$L=Na$ is the superlattice period, a is the lattice constant. If we are interested in the states derived only from the Γ or X states of the component materials, those $\psi_{\mathbf{k}_i}$ with $\mathbf{k}_i$ near the Γ or X points are necessary and sufficient to obtain convergent solutions.

With the empirical pseudopotential form factors of GaAs and AlAs given in Table I, we calculate the electronic subband of the superlattice $(GaAs)_{12}/(AlAs)_{12}$. The energy-band offsets ΔE_c and ΔE_v are adjusted so that the Γ- and lowest X-point energy levels cross in the case of no Γ-X mixing. Energies of the valence-band top E_v and of the conduction band at the Γ and X points, E_Γ and E_X, are listed in Table II, taking E_Γ of GaAs as zero. From Table II the ratio of the energy offsets is seen to be $\Delta E_c:\Delta E_v=69:31$.

The electronic subbands along k_x of $(GaAs)_{12}/(AlAs)_{12}$ are shown in Fig. 1, where the dashed lines are the Γ- and X-point energy levels calculated with the Bloch functions of $\mathbf{k}_i$ near the Γ or X points, respectively, and the solid lines are the energy levels calculated with the Bloch functions of all $\mathbf{k}_i$ in Eq. (2). Therefore, the former is the result ignoring the Γ-X mixing effect, and the latter is the result including the Γ-X mixing effect. From Fig. 1 the interaction and hybridization of the Γ and X states are seen clearly. In the case of ignoring the Γ-X mixing effect, the Γ- and X-point energy levels are parabolic functions of k_x, and the Γ level rises faster than the X levels due to the smaller effective mass of Γ electron. Because of the Γ-X mixing effect, the Γ- and X-point energy levels hybridize: the first level changes from Γ to X character, and the second level changes from X to Γ to X, etc., as k_x increases from zero to $0.5(2\pi/L)$. In Table III we give the Γ- and X-point energy levels E_Γ and E_X calculated ignoring Γ-X mixing, and the hybridized energy levels $E_{\Gamma X}$ calculated taking account of Γ-X mixing at $k=0$. The Γ and X components P_Γ and P_X of every hybridized state calculated by summation of the squared expansion coefficients C_{li}^2 in Eq. (1) over the $\mathbf{k}_i$ near Γ and X points, respectively, are also given in Table III. P_Γ and P_X represent quantitatively the extent of Γ-X mixing.

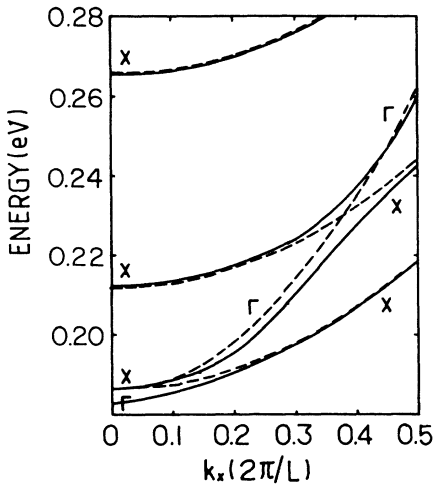

FIG. 1. Electronic subband along k_x of $(GaAs)_{12}/(AlAs)_{12}$ calculated with the pseudopotential method.

III. Γ-X MIXING EFFECT ON SUBBAND STRUCTURE STUDIED BY EFFECTIVE-MASS METHOD

Ando and Akero[4] presented the following boundary conditions for the envelope function in materials I and II to describe the Γ-X intervalley scattering:

$$\begin{aligned}
&\psi_\Gamma^{\mathrm{I}}=\psi_\Gamma^{\mathrm{II}} ,\\
&\psi_X^{\mathrm{I}}=\psi_X^{\mathrm{II}} ,\\
&\frac{a}{m_\Gamma^{\mathrm{I}*}}\frac{d\psi_\Gamma^{\mathrm{I}}}{dz}=\frac{a}{m_\Gamma^{\mathrm{II}*}}\frac{d\psi_\Gamma^{\mathrm{II}}}{dz}+t\psi_X^{\mathrm{II}} ,\\
&\frac{a}{m_X^{\mathrm{I}*}}\frac{d\psi_X^{\mathrm{I}}}{dz}=\frac{a}{m_X^{\mathrm{II}*}}\frac{d\psi_X^{\mathrm{II}}}{dz}+t\psi_\Gamma^{\mathrm{II}} ,
\end{aligned} \tag{3}$$

where a is the lattice constant, and $m_\Gamma^{\mathrm{I}*}$, $m_\Gamma^{\mathrm{II}*}$, $m_X^{\mathrm{I}*}$, and $m_X^{\mathrm{II}*}$ are the effective mass of Γ and X valley electrons in materials I and II, respectively. t, representing the extent of Γ-X mixing, is a parameter to be determined. It is noticed that Ando *et al.*[4] adopted opposite signs for t in the third and fourth equations of Eq. (3), which can be proved to be unphysical.

The electronic wave functions of Γ- and X-valley electrons can be written as

$$\begin{aligned}
\psi_\Gamma&=\sum_m \phi_\Gamma^{\mathrm{I}}(z-z_m)e^{i\chi z_m}+\sum_n \phi_\Gamma^{\mathrm{II}}(z-z_n)e^{i\chi z_n} ,\\
\psi_X&=\sum_m \phi_X^{\mathrm{I}}(z-z_m)e^{i\chi z_m}+\sum_n \phi_X^{\mathrm{II}}(z-z_n)e^{i\chi z_n} ,
\end{aligned} \tag{4}$$

where ϕ_Γ^{I}, $\phi_\Gamma^{\mathrm{II}}$, ϕ_X^{I}, and ϕ_X^{II} are the wave function of Γ- and X-point electrons, and z_m and z_n are the center coordi-

TABLE I. Pseudopotential form factors (in units of Ry) and lattice constants (in units Å) of GaAs and AlAs.

	$V^S(0)$	$V^S(3)$	$V^S(8)$	$V^S(11)$	$V^A(3)$	$V^A(4)$	$V^A(11)$	a
GaAs	0.0	−0.229	0.01	0.06	0.08	0.06	0.01	5.656
AlAs	−0.0215	−0.22	0.027	0.07	0.08	0.0625	−0.0075	5.656

TABLE II. Energies at special points of the Brillouin zone (in units of eV) and effective masses (in units of m_0) of GaAs and AlAs.

	E_v	E_Γ	E_X	m_Γ^*	m_X^*	$m_{X\parallel}^*$
GaAs	−1.5393	0.0	0.4125	0.081 52	2.8239	0.2491
AlAs	−2.0347	1.1094	0.1674	0.149 45	3.0482	0.2502

nates in materials I and II, respectively; χ is the wave vector along the z direction. $\phi_\Gamma^{\rm I}$, $\phi_\Gamma^{\rm II}$, $\phi_X^{\rm I}$, and $\phi_X^{\rm II}$ are propagating states or evanescent states depending on the electronic energy and the potential in each material. Letting the potential of the Γ-point electron in GaAs (I) and AlAs (II) be zero, and V_0, that of the X-point electron in GaAs and AlAs, be V_2 and V_1, respectively, from Table II we have $V_0 > V_2 > V_1$. Thus, the energy range of interest is $V_2 > E > V_1$ because only in this energy range can the bound X states exist in AlAs layers.

In this energy range $\phi_\Gamma^{\rm I}$, $\phi_\Gamma^{\rm II}$, $\phi_X^{\rm I}$, and $\phi_X^{\rm II}$ are of the forms

$$\begin{aligned}
\phi_\Gamma^{\rm I} &= A_{\rm I} e^{ikz} + B_{\rm I} e^{-ikz} , \\
\phi_\Gamma^{\rm II} &= A_{\rm II} e^{Kz} + B_{\rm II} e^{-Kz} , \\
\phi_X^{\rm I} &= C_{\rm I} e^{K'z} + D_{\rm I} e^{-K'z} , \\
\phi_X^{\rm II} &= C_{\rm II} e^{ik'z} + D_{\rm II} e^{-ik'z} ,
\end{aligned} \tag{5}$$

where

$$k = \left[\frac{2m_\Gamma^{\rm I*} E}{\hbar^2} \right]^{1/2} , \quad K = \left[\frac{2m_\Gamma^{\rm II*} (V_0 - E)}{\hbar^2} \right]^{1/2} ,$$

$$K' = \left[\frac{2m_X^{\rm I*} (V_2 - E)}{\hbar^2} \right]^{1/2} , \quad k' = \left[\frac{2m_X^{\rm II*} (E - V_1)}{\hbar^2} \right]^{1/2} . \tag{6}$$

From Eqs. (3)–(5), we obtain a set of linear homogeneous algebraic equations for $A_{\rm I}$, $B_{\rm I}$, $A_{\rm II}$, $B_{\rm II}$, $C_{\rm I}$, $D_{\rm I}$, $C_{\rm II}$, and $D_{\rm II}$ which has nontrivial solutions only if the coefficient determinant is equal to zero. Through a lengthy and tedious calculation we obtain the following eigenvalue equation:

$$\begin{aligned}
&-\{(1-\delta_1^2)\sin x_1 \sinh x_2 - 2\delta_1[\cos x_1 \cosh x_2 - \cos(\chi L)]\}\{(1-\delta_2^2)\sinh x_1' \sin x_2' + 2\delta_2[\cosh x_1' \cos x_2' - \cos(\chi L)]\} \\
&\quad + 2\varepsilon_1\varepsilon_2\{\delta_1 \sin x_1[\delta_2 \sinh x_1' + \sin x_2' \cos(\chi L)] - (\cosh x_2 + \cos x_1 \sinh x_2)(\delta_2 \sinh x_1' \cos x_2' + \cosh x_1' \sin x_2') \\
&\quad + \sinh x_2[\delta_2 \sinh x_1' \cosh(\chi L) + \sin x_2']\} + \varepsilon_1^2\varepsilon_2^2 \sin x_1 \sinh x_2 \sinh x_1' \sin x_2' = 0 ,
\end{aligned} \tag{7}$$

where

$$\begin{aligned}
\delta_1 &= \frac{m_\Gamma^{\rm I*} K}{m_\Gamma^{\rm II*} k} , \quad \delta_2 = \frac{m_X^{\rm I*} k'}{m_X^{\rm II*} K'} , \\
\varepsilon_1 &= \frac{t}{a} \frac{m_\Gamma^{\rm I*}}{k} , \quad \varepsilon_2 = \frac{t}{a} \frac{m_X^{\rm I*}}{K'} , \\
x_1 &= kd_1 , \quad x_2 = Kd_2 , \\
x_1' &= K'd_1 , \quad x_2' = k'd_2 .
\end{aligned} \tag{8}$$

d_1 and d_2 are the widths of GaAs (I) and AlAs (II) layers, respectively. The second term in Eq. (7) depends on ε_1 and ε_2, which come from the t in the third and fourth equations, respectively, of Eq. (3); hence the same or opposite sign for t will change the eigenvalue of energy drastically. In contrast, simultaneous change of t will not influence the results. Equations (8) can easily extend to the case of the wave vector parallel to the interface $k_\parallel$ not equal to zero, only taking the E in Eq. (6) as the longitudinal kinetic energy,

$$E_{\rm L} = E - \frac{\hbar^2 k_\parallel^2}{2m_\parallel^*} , \tag{9}$$

where $m_\parallel$ is the effective mass in the parallel direction,

TABLE III. Electronic energy levels without Γ-X mixing, E_Γ and E_X (relative to the conduction-band bottom of GaAs, in units of meV), that with Γ-X mixing, $E_{\Gamma X}$, energy shifts $\Delta E = E_{\Gamma X} - E_\Gamma$ (or E_X), and Γ and X components in every state P_Γ and P_X for superlattice $(\text{GaAs})_{12}/(\text{AlAs})_{12}$ at $\mathbf{k}=\mathbf{0}$.

E_Γ	186.21				
E_X		186.22	211.81	266.22	331.90
$E_{\Gamma X}$	182.83	186.67	212.37	265.84	332.42
ΔE	−3.38	0.45	0.56	−0.38	0.52
P_Γ	0.8291	0.1289	0.0289	0.0066	0.0091
P_X	0.1709	0.8711	0.9711	0.9934	0.9909

which is different from that in the perpendicular direction for the X-point electron.

With the values of V_0, V_1, and V_2, and m_Γ^{I*}, m_Γ^{II*}, m_X^{I*}, m_X^{II*}, $m_{X\|}^{I*}$, and $m_{X\|}^{II*}$, calculated from the pseudopotential calculation for the energy bands of GaAs and AlAs (given in Table II) and $d_1=d_2=33.94$ Å, we calculated the Γ and X subbands for $t=0$ and the hybridized subbands in the existence of Γ-X mixing ($t\neq 0$). Compared with results of the pseudopotential calculation, we have determined the best-fitting parameter t to be 0.5. With this value for t, the calculated subbands are shown in Fig. 2, and the results paralleling those of Table III are given in Table IV. From Figs. 1 and 2 and Tables III and IV, we see that the results derived from the two completely different models are in reasonable agreement.

Finally we consider the problem of the sign of t in Eq. (3). The boundary conditions (3) can be derived by a δ-function potential at the interface. If we use a two-component function $\begin{pmatrix}\psi_\Gamma(z)\\ \psi_X(z)\end{pmatrix}$ to represent the electronic wave function, the electronic Hamiltonian can be written as

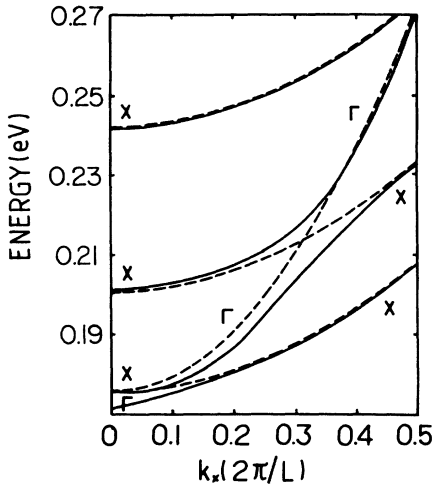

FIG. 2. Electronic subband along k_x of $(GaAs)_{12}/(AlAs)_{12}$ calculated with the effective-mass equation (3) for $t=0.5$.

$$H_e=\begin{bmatrix} -\frac{1}{2m_\Gamma^*}\frac{d^2}{dz^2}+V_\Gamma(z) & \frac{t_1}{2a}[\delta(z-d/2)-\delta(z+d/2)] \\ \frac{t_2}{2a}[\delta(z-d/2)-\delta(z+d/2)] & -\frac{1}{2m_X^*}\frac{d^2}{dz^2}+V_X(z)\end{bmatrix}, \tag{10}$$

where the nondiagonal terms represent the Γ-X scattering, $V_\Gamma(z)$ and $V_X(z)$ are the effective potentials of Γ- and X-point electrons, respectively, and $d/2$ and $-d/2$ are the interface coordinates. Assuming that $\psi_\Gamma(z)$ and $\psi_X(z)$ are the wave functions of Γ- and X-point electrons for $t_1=t_2=0$, the matrix elements of Γ-X interaction are

$$H_{12}=\frac{t_1}{2a}[\psi_\Gamma^*(d/2)\psi_X(d/2)-\psi_\Gamma^*(-d/2)\psi_X(-d/2)]\,,$$
$$H_{21}=\frac{t_2}{2a}[\psi_X^*(d/2)\psi_\Gamma(d/2)-\psi_X^*(-d/2)\psi_\Gamma(-d/2)]\,. \tag{11}$$

From the condition that the Hamiltonian should be Hermitian, $H_{12}=(H_{21})^*$, we obtain $t_1=t_2$, not $t_1=-t_2$.

IV. Γ-X MIXING EFFECT IN RESONANT TUNNELING

The resonant tunneling of heterojunctions taking account of the Γ-X mixing effects was studied by a method similar to that used in studying the hole resonant tunneling.[14] Assuming that electrons transport through the potential barrier and well region from left to right in the energy range $V_2>E>V_1$, the electronic wave function at the left- and right-hand side can be written as

$$\psi_l=\alpha\psi_{\Gamma,k}+\beta\psi_{\Gamma,-k}+\gamma\psi_{X,K}+\delta\psi_{X,-K}\,,$$
$$\psi_r=\alpha'\psi_{\Gamma,k}+\beta'\psi_{\Gamma,-k}+\gamma'\psi_{X,K}+\delta'\psi_{X,-K}\,, \tag{12}$$

respectively, where k and K are given in Eq. (6). In the case of applied voltage, the k and K in the ψ_l and ψ_r of Eq. (11) will be different. The coefficients $(\alpha,\beta,\gamma,\delta)$ and $(\alpha',\beta',\gamma',\delta')$ are connected by a transfer matrix $\underline{M}$,

$$\begin{pmatrix}\alpha\\ \beta\\ \gamma\\ \delta\end{pmatrix}=\underline{M}\begin{pmatrix}\alpha'\\ \beta'\\ \gamma'\\ \delta'\end{pmatrix}. \tag{13}$$

The transmission and reflection amplitudes for the Γ-

TABLE IV. Same as Table I, but calculated with effective-mass Eq. (3) for $t=0.5$.

E_Γ	175.26				
E_X		175.81	200.86	242.00	297.97
$E_{\Gamma X}$	175.51	175.75	201.78	241.43	298.42
ΔE	−3.75	−0.06	0.92	−0.57	0.45
P_Γ	0.9550	0.0001	0.0342	0.0010	0.0077
P_X	0.0450	0.9999	0.9658	0.9990	0.9923

point electron can be proved to be

$$T=\frac{\underline{M}_{44}}{\underline{M}_{11}\underline{M}_{44}-\underline{M}_{14}\underline{M}_{41}}\ ,$$
$$R=\frac{\underline{M}_{21}\underline{M}_{44}-\underline{M}_{24}\underline{M}_{41}}{\underline{M}_{11}\underline{M}_{44}-\underline{M}_{14}\underline{M}_{41}}\ . \tag{14}$$

For a single barrier of AlAs (here and after the "barrier" only refers to the Γ-point electron; for the X-point electron we will be referring to a potential well) and no electric field, the transmission probability can be calculated by use of the boundary conditions (3),

$$T^*T=\frac{|\underline{M}_{44}|^2}{\mathcal{C}_R^2+\mathcal{C}_I^2}\ , \tag{15}$$

where

$$|M_{44}|=\frac{1}{2}\left[2\cosh(k'd)-\left[\delta_2-\frac{1}{\delta_2}\right]\sin(k'd)-\left[\frac{t}{a}\right]^2\frac{m_\Gamma^{II*}}{K}\frac{m_X^{I*}}{K'}\sinh(Kd)\right]\ ,$$
$$\mathcal{C}_R=\cosh(Kd)\left[\cos(k'd)-\frac{1}{2}\left[\delta_2-\frac{1}{\delta_2}\right]\sin(k'd)\right]-\frac{1}{2}\left[\frac{t}{a}\right]^2\frac{m_\Gamma^{II*}}{K}\frac{m_X^{I*}}{K'}\sinh Kd\left[\cos(k'd)+\frac{1}{\delta_2}\sin(k'd)\right]\ , \tag{16}$$
$$\mathcal{C}_I=\frac{1}{4}\left\{\left[\delta_1-\frac{1}{\delta_1}\right]\sinh(Kd)\left[2\cos(k'd)-\left[\delta_2-\frac{1}{\delta_2}\right]\sin(k'd)\right]\right.$$
$$+2\left[\frac{t}{a}\right]^2\frac{m_\Gamma^{I*}}{k}\frac{m_X^{I*}}{K'}\left[1-\cosh(Kd)\left[\cos(k'd)+\frac{1}{\delta_2}\sin(k'd)\right]\right]$$
$$\left.+\left[\frac{t}{a}\right]^4\frac{m_\Gamma^{I*}}{k}\frac{m_\Gamma^{II*}}{K}\frac{m_X^{I*}}{K'}\frac{m_X^{II*}}{k'}\sin(k'd)\sinh(Kd)\right\}\ ,$$

and d is the width of the potential barrier.

For the case of double barriers and applied voltage, the problem becomes very complicated and can only be solved by numerical integration,[14] taking into account the discontinuity of the differential of wave functions at the interface [Eqs. (3)]. The results of the numerical integration are in agreement with the analytical results of Eq. (15) for the simple case.

Taking the same parameters as in Sec. III, we calculated the transmission probabilities of Γ-point electron as functions of energy for the single and double barriers, and for parallel wave vector $k_\parallel=0$ and $0.4(2\pi/L)$. The results are shown in Figs. 3–5. All the resonant peaks correspond to the stationary states of superlattices shown in Fig. 2. For the single barrier, there is no Γ-resonant peak, and the peak-to-valley ratios are smaller than that in double barriers by about a factor of 3. It is surprising that the X-resonant peaks are higher and larger than the Γ-resonant peak, though the Γ-X scattering parameter t is not too large. Figure 6 shows the transmission proba-

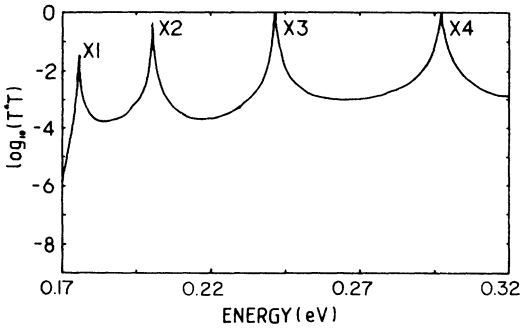

FIG. 3. Transmission probabilities as function of energy for single barrier and $\mathbf{k}_\parallel=\mathbf{0}$.

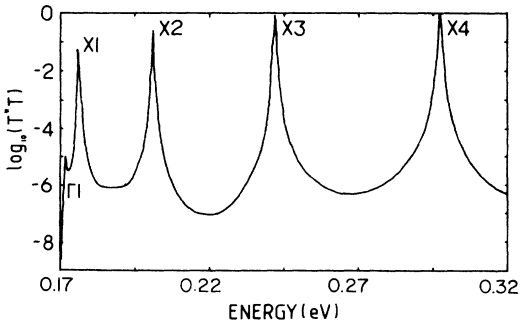

FIG. 4. Transmission probabilities as function of energy for double barriers and $\mathbf{k}_\parallel=\mathbf{0}$.

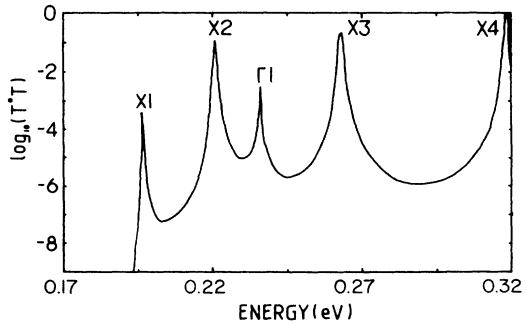

FIG. 5. Transmission probabilities as function of energy for double barriers and $k_x=0.4(2\pi/L)$.

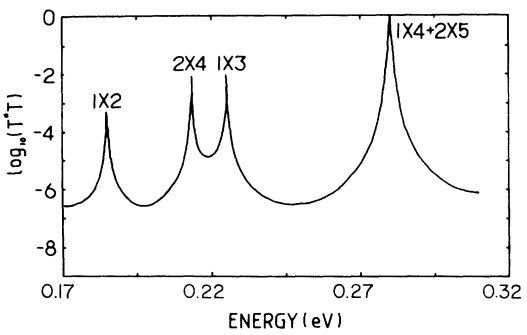

FIG. 6. Transmission probabilities as function of energy for double barriers and $\mathbf{k}_{\parallel}=\mathbf{0}$, under an applied electric field of 1 mV/Å.

bilities in the applied electric field $F=1$ mV/Å for the double barriers. The results can be easily understood by the energy-band profile in the electric field (Fig. 7), in which all the bound energy levels in each material are shown. The 1×2, 1×3, and 1×4 states in the first barrier and the 2×4 and 2×5 states in the second barrier take part in the resonant process. The double peaks in Fig. 7 come from 1×3 and 2×4 states, and the large single peak is the result of the coincidence of the two resonant peaks, 1×4 and 2×5. The resonant tunneling through X-bound states has the following character: the spacing between the X-resonant peaks is much smaller than that between Γ-resonant peaks, in the X-resonant region the Γ-resonant peak is smaller than the X-resonant peak, the energy dispersion in the $k_{\parallel}$ direction is larger because $m^*_{X\parallel} \ll m^*_X$ (see Table II), and in the applied electric field the X-resonant peaks from two barriers separate. All these factors reduce the peak-to-valley ratios and make it difficult to observe the negative differential resistances caused by the X-resonant states in AlAs layers.

In conclusion, we investigated the Γ-X mixing effect on the subband structure of superlattice $(GaAs)_{12}/(AlAs)_{12}$

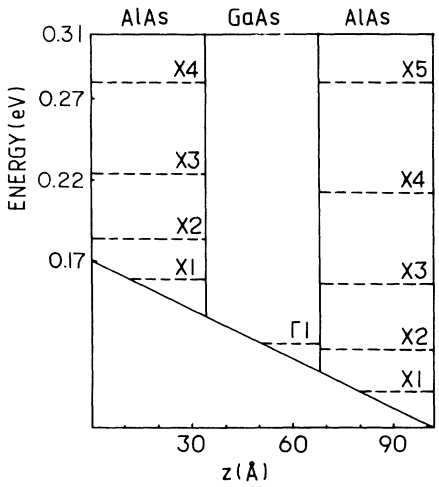

FIG. 7. Energy-band profile for the double barriers AlAs/GaAs/AlAs under an applied electric field of 1 mV/Å.

by both the pseudopotential method and the effective-mass method. The results derived from the two methods show reasonable agreement, and by comparison of the results the best-fitting Γ-X scattering parameter t is determined to be 0.5. The transmission probabilities of the Γ-point electron through the bound X states in AlAs layers are calculated quantitatively. It is found that the resonant peaks correspond completely to the eigenstates of corresponding superlattices, and the Γ-resonant peak is relatively smaller than the X-resonant peaks. In the applied electric field the resonant peaks originating from two barriers separate, resulting in a reduction of peak-to-valley ratio.

ACKNOWLEDGMENTS

This work was supported by the Chinese National Science Foundation.

[1]E. E. Mendez, E. Calleja, C. E. T. Gonçalves da Silva, L. L. Chang, and W. I. Wang, Phys. Rev. B **33**, 7368 (1986).
[2]G. C. Osbourn, J. Vac. Sci. Technol. **19**, 592 (1981).
[3]C. Maihiot, T. C. McGill, and J. N. Schulman, J. Vac. Sci. Technol. B **1**, 439 (1983).
[4]T. Ando and H. Akera, in *Proceedings of the Nineteenth International Conference on the Physics of Semiconductors,* edited by W. Zawadzki (Institute of Physics, Polish Academy of Sciences, Warsaw, 1988), p. 603.
[5]J. N. Schulman and Y. C. Chang, Phys. Rev. B **31**, 2056 (1985).
[6]M. A. Gell and M. Jaros, Superlatt. Microstruct. **3**, 121 (1987).
[7]J.-B. Xia, Phys. Rev. B **38**, 8358 (1988).
[8]G.-H. Li D.-S. Jiang, H.-X. Han, Z.-P. Wang, and K. Plogg, Phys. Rev. B **40**, 10430 (1989).
[9]Y.-T. Lu and L. J. Sham, Phys. Rev. B **40**, 5567 (1989).
[10]A. R. Bonnefoi, T. C. McGill, and R. D. Burnham, Phys. Rev. B **37**, 8754 (1988).
[11]P. M. Solomon, S. L. Wright, and C. Lanza, Superlatt. Microstruct. **2**, 521 (1986).
[12]P. J. Price, Surf. Sci. **196**, 394 (1988).
[13]J.-B. Xia, Phys. Rev. B **39**, 3310 (1989).
[14]J.-B. Xia, Phys. Rev. B **38**, 8365 (1988).